ELSEVIER

The Journal of Heart and Lung Transplantation

http://www.jhltonline.org

An electrically coupled tissue-engineered cardiomyocyte scaffold improves cardiac function in rats with chronic heart failure

Jordan J. Lancaster, MS,[a,b,c] Elizabeth Juneman, MD,[a,b] Sarah A. Arnce, MMS, PA-C,[a,b] Nicholle M. Johnson, BS,[a,b] Yexian Qin, PhD,[d] Russell Witte, PhD,[d] Hoang Thai, MD,[a,b] Robert S. Kellar, PhD,[e] Jose Ek Vitorin, PhD, MD,[c] Janis Burt, PhD,[c] Mohamed A. Gaballa, PhD,[f] Joseph J. Bahl, PhD,[a,b] and Steven Goldman, MD[a,b]

From [a]Cardiology and Medicine, Southern Arizona VA Health Care System; the [b]Sarver Heart Center; the [c]Department of Physiology; and [d]Medical Imaging, University of Arizona, Tucson; [e]Northern Arizona University, Flagstaff; and the [f]Banner Sun Health Research Institute, Sun City, Arizona.

KEYWORDS:
chronic heart failure;
ventricular function;
ventricles;
ejection fraction;
cardiomyocytes;
cell therapy

BACKGROUND: Varying strategies are currently being evaluated to develop tissue-engineered constructs for the treatment of ischemic heart disease. This study examines an angiogenic and biodegradable cardiac construct seeded with neonatal cardiomyocytes for the treatment of chronic heart failure (CHF).

METHODS: We evaluated a neonatal cardiomyocyte (NCM)-seeded 3-dimensional fibroblast construct (3DFC) in vitro for the presence of functional gap junctions and the potential of the NCM-3DFC to restore left ventricular (LV) function in an in vivo rat model of CHF at 3 weeks after permanent left coronary artery ligation.

RESULTS: The NCM-3DFC demonstrated extensive cell-to-cell connectivity after dye injection. At 5 days in culture, the patch contracted spontaneously in a rhythmic and directional fashion at 43 ± 3 beats/min, with a mean displacement of 1.3 ± 0.3 mm and contraction velocity of 0.8 ± 0.2 mm/sec. The seeded patch could be electrically paced at nearly physiologic rates (270 ± 30 beats/min) while maintaining coordinated, directional contractions. Three weeks after implantation, the NCM-3DFC improved LV function by increasing ($p < 0.05$) ejection fraction 26%, cardiac index 33%, dP/dt(+) 25%, dP/dt(–) 23%, and peak developed pressure 30%, while decreasing ($p < 0.05$) LV end diastolic pressure 38% and the time constant of relaxation (Tau) 16%. At 18 weeks after implantation, the NCM-3DFC improved LV function by increasing ($p < 0.05$) ejection fraction 54%, mean arterial pressure 20%, dP/dt(+) 16%, dP/dt(–) 34%, and peak developed pressure 39%.

CONCLUSIONS: This study demonstrates that a multicellular, electromechanically organized cardiomyocyte scaffold, constructed in vitro by seeding NCM onto 3DFC, can improve LV function long-term when implanted in rats with CHF.

J Heart Lung Transplant 2014;33:438–445

Chronic heart failure (CHF) is the leading cause of morbidity and mortality worldwide. Although current medical therapeutics decrease mortality from CHF, they do not reverse the disease process or restore long-term

Reprint requests: Jordan J. Lancaster, MS, Cardiology Section, 1-111C; SAVAHCS, 3601 S 6th Ave, Tucson, AZ 85723. Telephone: 520-792-1450, ext 6319. Fax: 520-629-4636.

E-mail address: jordan.lancaster@va.gov

1053-2498/$ - see front matter
http://dx.doi.org/10.1016/j.healun.2013.12.004

cardiac function. Recently, a number of novel strategies have been proposed for improving functional and clinical outcomes of patients with CHF such as, cell-based therapies,[1] in vivo tissue reprogramming,[2] and gene therapy.[3] Each of these approaches may carry therapeutic potential, but cell-based therapies offer the least cumbersome approach and are not complicated by in vivo viral or gene administration.

Evaluation of cell-based therapies for CHF has progressed through a number of clinical trials.[4–10] Although questions remain regarding the most effective cell type and dosing strategies, the major limitation to success may be the development of an effective cell-delivery system. Current delivery techniques, for the most part, use direct injection by catheter-based systems that result in limited cellular survival and minimal retention of cells in the target area.[11,12] As a result, new cell-delivery strategies, such as tissue engineered constructs, are being developed that provide structural support facilitating implanted cell survival and integration into the underlying myocardium.[13–15]

Previous studies by our laboratory, and others, have tested a 3-dimensional fibroblast construct (3DFC) consisting of viable human dermal fibroblasts embedded onto a bioabsorbable polymeric Vicryl mesh (Ethicon, Somerville, NJ) that does not elicit an immunologic response.[16–18] Implantation of this 3DFC immediately after myocardial infarction (MI) or in an ischemic CHF model, 3 weeks after permanent occlusion of the left coronary artery, results in formation of a microvascular bed and the consequent increase in myocardial blood flow to the infarcted tissue.[19,20] The embedded fibroblasts are an important component of the bioengineered scaffold because dermal fibroblasts have been demonstrated to play a role in microvascular organization in vitro through paracrine-mediated effects or other factors.[21–23] Yet, implanting the 3DFC alone in CHF did not improve cardiac function.[19,20]

In the present study, we explored the potential of the microvascular bed induced by the 3DFC to support an overlaying population of cardiomyocytes seeded on the 3DFC. We demonstrate that rat neonatal cardiomyocytes (NCM) can be successfully cocultured with human fibroblasts in a biodegradable scaffold and that they form an electromechanically organized syncytium capable of improving the left ventricular (LV) function of a chronically infarcted heart.

Methods

The 3DFC

The 3DFC is a cryopreserved bioabsorbable scaffold populated with human neonatal fibroblasts.[16,17] The fibroblasts have been tested for cell morphology, karology, isoenzymes, and tumorigenicity and are free from viruses, retroviruses, endotoxins, and mycoplasma. The 3DFC was provided by Theregen Inc (San Francisco, CA) frozen (–75° ± 10°C) in 5 × 7.5 cm pieces with an average thickness of 200 μm. The 3DFC is thawed in phosphate buffered saline (34°C–37°C) and handled gently to limit cellular damage. The 3DFC does not generate an immune response[16–20] (investigators' brochure ITT-101, Theregen).

Cardiomyocyte isolation, seeding, and culture

Cardiomyocytes were isolated from 1- to 2-day-old neonatal Sprague-Dawley (Harlan, Indianapolis, IN) rat hearts. Briefly, the hearts were excised, the atria were removed, and the ventricles were minced into 0.5- to 1-mm portions and digested in a pancreatin/collagenase solution. After each enzymatic digest, cardiomyocytes were collected, combined, and resuspended in Dulbecco Modified Eagle's medium (DMEM) with 10% fetal bovine serum (FBS). Lastly, the suspension was differentially plated in Ham's F-12 with 100 mg/ml bovine serum albumin.

The 3DFC was thawed, cut into 1.5-cm diameter sections, and seeded with NCM at densities ranging from 0.6×10^6 to 2.7×10^6 cells/cm^2 using methods developed in our laboratory. The NCM and NCM-3DFC were cultured in 10% FBS in DMEM-LG (Gibco-Invitrogen, Carlsbad, CA), maintained at 37°C and 5% CO_2. Patches were constructed as described for in vitro and in vivo evaluation. The NCM-3DFC patches for in vivo evaluation were seeded, cultured, and implanted onto the rat heart 3 weeks after left coronary artery ligation within 18 hours of seeding. Patches prepared for in vitro evaluation were seeded and cultured 1 to 10 days.

Quantitative measurements of cardiomyocytes and fibroblasts

Serial stained tissue samples were reacted with specific markers for cardiomyocytes (troponin) and fibroblasts (vimentin). Immunohistochemically reacted glass slides were digitally scanned (whole-slide scanning) using an Aperio scanner (Aperio, Vista, CA), with subsequent FACTS (Feature Analysis on Consecutive Tissue Sections). Whole-slide scanning allowed for an objective digital quantitative analysis of the entire tissue sections to ensure against investigator bias. The parameters for a generic image analysis algorithm for quantifying cells were independently adjusted for counting cardiomyocytes and fibroblasts. This was used for the objective analysis. The algorithm-based FACTS process performs image-to-image registration on prepared tissue sections on each glass slide. The FACTS process was used to align the serial sections to ensure that corresponding areas were analyzed in each stained slide to provide a fair sample comparison.

Field stimulation and pacing

NCM-seeded 3DFC patches were transferred to a thermoregulated culture well (Bipolar Temperature Controller; Medical Systems, Greenvale, NY) containing culture medium maintained at 37°C. The NCM-3DFC were paced (S44; Grass Instruments, Quincy, MA) by field stimulation (~7 V) through 99.7% pure silver wires placed into the culture well on opposing sides of the NCM-3DFC. The pacing rate varied from 60 to 270 ± 30 beats/min for 10 seconds.

Cell-to-cell communication

Functional gap junction formation was examined in 3DFC, NCM-3DFC, and halothane-treated NCM-3DFC patches at 6 days. Three dyes were injected simultaneously: [2-(4-nitro-2,1,3-benzoxadiol-7-yl)aminoethyl]trimethylammonium (NBD-TMA [provided by

Dr Steve Wright, University of Arizona, Tucson, AZ][24]; mol wt 280, net charge 1+, 10 mmol/liter), Alexa 350 (mol wt 326, net charge 1–, 10 mmol/liter), and rhodamine dextran (0.1 mg/ml; both Molecular Probes; Invitrogen, Carlsbad, CA).

Microelectrode tips were created from 1.0-mm filament glass (A-M Systems, Sequim, WA) on a Sutter Instruments puller (Novato, CA), their tips filled by capillary action with the dye mixture and backfilled with 3 mol/liter KCl. The microelectrodes were lowered onto a cell field in the preparation until contact with a cell surface was achieved and cytoplasm access was gained. The dyes were slowly and continuously injected by a slight capacitance overcompensation of the amplifier (SEC-05LX; NPI Electronics, Tamm, Germany). Images were captured at different times during the next 5 to 20 minutes. Halothane, a known gap junction inhibitor, was added to the superfusate (final concentration, ~8 mmol/liter) to temporarily decrease intercellular dye diffusion and further confirm the transjunctional nature of this phenomenon.[25–27]

Multielectrode array electrical mapping

The NCM-3DFC was electrophysiologically mapped in real-time using a 10-electrode custom-designed multielectrode array (Ad-Tech Medical Instrument Corp, Racine, WI) and a 1-kHz low-pass filter. Action potentials were collected using a BIOPAC MP150 (BIOPAC Systems Inc, Goleta, CA) data acquisition system with MCE100C signal conditioning modules. The MCE module has multiple gain settings from 10 to 1,000 and an on-board configurable signal filter. Up to 16 channels of data were acquired simultaneously at a 5-kHz sampling rate. Notch filters were configured in the data acquisition system for removing the 60 Hz noise and its higher harmonics. Data recordings were collected in 10-second intervals. Seeded patches were evaluated in vitro at 1 to 8 days in culture for spontaneous field potential amplitude, duration, conduction velocities, propagation patterns, and monophasic action potentials. The NCM-3DFC was maintained at 37°C in standard culture medium.

Coronary artery ligation experimental CHF

All animals in this study received humane care in compliance with the "Principles of Laboratory Animal Care" and the "Guide for the Care and Use of Laboratory Animals." The rat coronary artery ligation model is standard in our laboratory.[28–30] In brief, Sprague-Dawley rats were anesthetized with ketamine and acepromazine and underwent a left thoracotomy. The heart was expressed from the thorax and a ligature placed around the proximal left coronary artery.

The rats were maintained post-operatively on standard rat chow, water ad libitum, and pain medication. Only rats with an ejection fraction (EF) of $\leq$ 35% after permanent left coronary artery ligation at 3 weeks post-MI were enrolled in the study. Three weeks after MI, the chest was reopened, and the NCM-3DFC was implanted with suture on the infarcted ventricle bridging to viable myocardium.

Echocardiography

Closed-chest transthoracic echocardiography was performed using a Vingmed, Vivid 7 system echo machine with EchoPac (both GE Ultrasound, Fairfield, CT) programming software with a 10-MHz multiplane transducer, with views in the parasternal short-axis and long-axis, to evaluate the anterior, lateral, anterolateral, inferior, and posterior walls. Systolic displacement of the anterior wall and EF were obtained from 2D and M-mode measurements of myocardial wall thickness and LV dimensions.[19,31]

Hemodynamic measurements in vivo

Rats were anesthetized with a 100 mg/kg intraperitoneal injection of Inactin (Sigma-Aldrich, St. Louis, MO), intubated, and placed on a rodent ventilator with a 2F solid-state micromanometer-tipped catheter with 2 pressure sensors (Millar Instruments Inc, Houston, TX) inserted through the carotid artery. One sensor was located in the LV and another in the ascending aorta. The pressure sensor was equilibrated in 37ºC saline, and LV and aortic pressures/heart rate were recorded and digitized at a rate of 1,000 Hz to calculate LV dP/dt and the time constant (Tau) of LV relaxation.[19,25–29] Hemodynamic measurements were obtained at the end of the study, 6 weeks post-MI (3 weeks post-implantation of 3DFC), and 21 weeks post-MI (18 weeks post-implantation).

Statistical analysis

Data are expressed as mean ± standard error (SE). Student's *t*-test was used for single comparison of group vs group analysis of statistical significance ($p < 0.05$).

Results

Cardiomyocyte seeding

Cardiomyocyte seeding densities were evaluated between 0.6 and 2.7 $\times$ 10^6 cells/cm^2. Lower-density cardiomyocyte preparations (0.6 to 1.2 $\times$ 10^6 cells/cm^2) displayed spontaneous, non-synchronized contractions after 48 hours in tissue culture. At 72 hours, these contractions began synchronizing, and by 84 hours, cell contractions were fully synchronized. Higher density cardiomyocyte preparations (1.8 to 2.7 $\times$ 10^6 cells/cm^2) displayed synchronized and spontaneous contractions of the entire scaffold after 48 hours in tissue culture (Video 1, available on the jhltonline.org Web site).

Contractions increased in robustness from 48 hours to 5 days. At day 5, scaffolds seeded with 2.7 $\times$ 10^6 cells/cm^2 contracted in a consistent rhythmic and directional fashion. NCMs plated in 35-mm^2 plates (control) displayed contractions at 97 ± 4 beats/min, whereas NCM-3DFC was recorded at 43 ± 3 beats/min (Supplementary Figures 1 and 2, available on the jhltonline.org Web site) with a mean displacement of 1.3 ± 0.3 mm (Supplementary Figure 3, available on the jhltonline.org Web site) and a contraction velocity of 0.8 ± 0.2 mm/sec ($n = 10$; Supplementary Figure 4, available on the jhltonline.org Web site).

In vitro cellular composition

In vitro quantification of the cellular composition of the NCM-3DFC showed a fibroblast nuclear density ($n = 5$) of 931 ± 72 and 974 ± 95 nuclei/mm^2 and a cardiomyocyte nuclear density ($n = 4$) of 5,808 ± 527

and 4,923 ± 287 nuclei/mm^2 at 2 and 8 days in culture, respectively. Thus, a 5:1 ratio of myocyte to fibroblast nuclear density and no cell loss were found between 2 and 8 days in culture.

Field stimulation

External field stimulation was applied to the NCM-3DFC at varying culture time points (2–6 days) in temperature-controlled (37°C) wells. The NCM-3DFC contracted synchronously (Video 2, available on the jhltonline.org Web site) when paced for 20-second intervals at physiologic rates up to 270 ± 30 beats/min.[32]

Cell-to-cell communication

Dye injections into the fibroblasts of the 3DFC alone resulted in no detectable transjunctional diffusion (Figure 1A). In contrast, dye diffusion readily occurred from the injected myocytes toward neighboring cells on the NCM-3DFC (Figure 1B; Video 3, available on the jhltonline.org Web site). Furthermore, as can be expected from the gradual organization of cell bundles, junctional connectivity increased from Day 2 through 6 days (data not shown). When the NCM-3DFCs were exposed to halothane, dye was retained in the donor cell, reaching higher concentrations but failing to diffuse to the neighboring cells despite the obvious intercellular gradient (Figure 1C).

Electrical mapping

The spontaneous electrical activation of the NCM-3DFC was mapped by electrically recording constructs at varying times in tissue culture. The NCM-3DFC yielded maximum and minimum transverse conduction voltage amplitude of 42 μV and –75 μV, respectively. A consistent sequence of transverse activation was seen beat-to-beat (Figure 2; Video 4, available on the jhltonline.org Web site).

Hemodynamics and echocardiography

At 3 weeks after implantation, the NCM-3DFC increased ($p < 0.05$) EF from 31% ± 2% to 39% ± 1% (Figure 3), cardiac index from 0.46 ± 0.05 to 0.61 ± 0.06 ml/(g min), dP/dt(+) from 4,651 ± 250.4 to 5,806.2 ± 192.1 mm Hg/sec, dP/dt(–) from 2,852.9 ± 147.7 to 3,516.9 ± 229.5 mm Hg/sec, and peak developed pressure (PDP) from 112.2 ± 7.6 to 146.4 ± 5.4 mm Hg (Table 1), while decreasing ($p < 0.05$) LV end diastolic pressure from 24 ± 2 to 15 ± 3 mm Hg and Tau from 24.9 ± 1.2 to 20.9 ± 1.1 msec (Table 1). At 18 weeks post-implantation, the NCM-3DFC improved LV function by increasing ($p < 0.05$) EF from 21.8% ± 2.8% to 33.6% ± 4.1% (Figure 3), MAP from 84.3 ± 1.7 to 101 ± 2.9 mm Hg, dP/dt(+) from 4047.7 ± 216.6 to 4713.0 ± 118.4 mm Hg/sec, dP/dt(–) from 2,172.3 ± 130.2 to 2,915.3 ± 218.6 mm Hg/sec, and PDP from 98.3 ± 9 to 137.3 ± 5 mm Hg (Table 2). Importantly, the rats maintained normal sinus rhythm throughout the entire study, and the echocardiography revealed

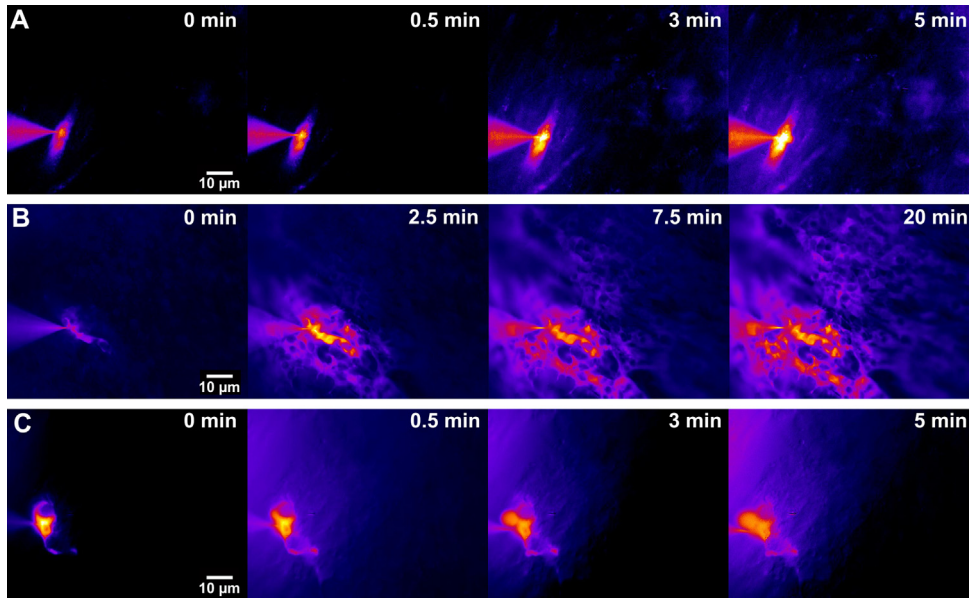

Figure 1 Time elapsed images (original magnification ×40) of (A) 3-dimensional fibroblast construct (3DFC), (B) neonatal cardiomyocyte (NCM)-3DFC, and (C) NCM-3DFC treated with halothane at day 6 of culture. In all images, the dye-filled electrode is at the left, and its tip allows the location of the injected cell (donor). From this cell, dye may diffuse across gap junctions to other (recipient) cells. The dye [2-(4-nitro-2,1,3-benzoxadiol-7-yl)aminoethyl]trimethylammonium (NBD) easily occupies the cytoplasmic space, but does not penetrate the nucleus; thus, individual recipient cells can be located by the image of NBD fluorescence surrounding a central, less fluorescent area. (A) No detectable intercellular dye transfer occurs from the injected fibroblast to neighboring cells. (B) The dye injected into a single NCM spreads through established gap junctions toward neighboring cells. (C) After halothane treatment, a transient decrease on the speed of transjunctional dye diffusion was observed. In this particular image, the reflection of the highly concentrated dye in the injected cell is perceived, but only 1 recipient cell (adjacent to the injected one) can be clearly identified after 5 minutes.

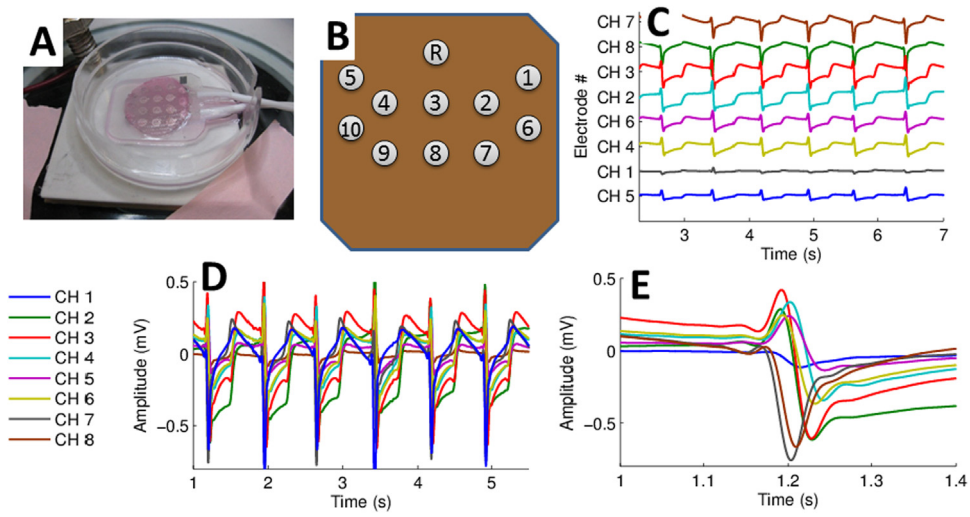

Figure 2 (A) Electrical activation mapping was performed on the neonatal cardiomyocyte (NCM)-3-dimensional fibroblast construct (3DFC) in tissue culture 5 days after coculturing using a custom designed multielectrode array with 18 recording sites spaced 500 μm apart. (B) Recordings were performed from 10 electrodes; each recording site was numbered sequentially as channel 1–10. (C) The electrical activation of the patch shows consistent beat-to-beat activation, as shown in 7-second interval displaying the peak transverse conduction voltage for each individual channel. The amplitude is shown (D) with all channels superimposed in a beat-to-beat sequence and (E) during a single activation. The amplitude was recorded as (D) 0.03 to 0.42 and (E) –0.13 to –0.75 mV (E).

the previously infarcted area contracted in sync with the rest of the heart, with no arrhythmias and no evidence of dyssynchrony.

LV cross sections

As shown in Figure 4, implantation of the NCM-3DFC is well tolerated, and within 3 weeks of implantation, the synthetic Vicryl components have degraded and are not visible. As shown by echocardiography and hemodynamic values, implantation of the NCM-3DFC results in improvements of cardiac function. This may be partly due to the effective integration of the transplanted myocytes, or alternatively, enhanced survival/migration/function of endogenous myocardium under the implant. In either case, an increased presence of myocytes in or around the infarcted area was observed (Figure 4).

Discussion

The present report demonstrates NCMs can be seeded and cocultured onto the 3DFC, resulting in cardiac patches that in vitro contract spontaneously in a rhythmic, synchronous manner in culture (Video 1, available on the jhltonline.org Web site) and are cable of being electrically paced when subject to electrical field stimulation (Video 2, available on the jhltonline.org Web site). We confirmed the existence of functional gap junctions by cell-to-cell diffusion of permeant dye across the patch (Video 3, available on the jhltonline.org Web site; Figure 1B) and were further validated by transient gap junction inhibition with halo thane,[25–27] effectively blocking dye passage (Figure 1C). Furthermore, electrical mapping of the NCM-3DFC with a multielectrode array system demonstrated consistent beat-to-beat electrical activation and cellular coupling (Video 4, available on the jhltonline.org Web site; Figure 2). Quantita tive evaluation of cellular composition showed no loss of cells during tissue culture between 2 and 8 days. These findings support the 3DFC as a suitable construct to support cardiomyocytes and permit structural organization of the

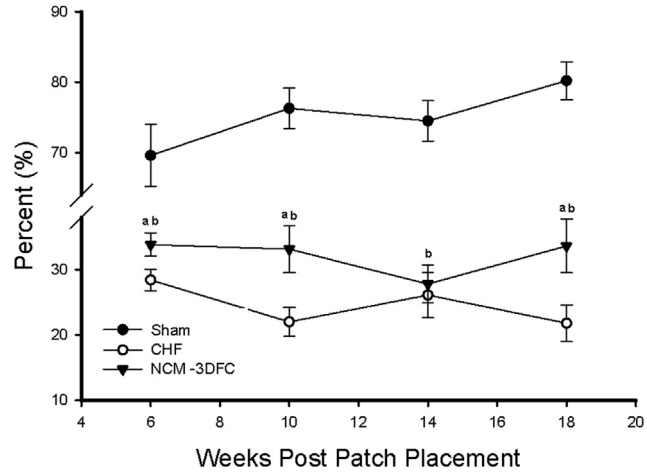

Figure 3 Echocardiography evaluation of ejection fraction in rats with chronic heart failure (CHF) at 6, 10, 14, and 18 weeks after patch implantation. Implantation of the neonatal cardiomyocyte (NCM)–3-dimensional fibroblast construct (3DFC) improves ejection fraction at 6 ($p = 0.037$), 10 ($p = 0.015$), and 18 ($p = 0.046$) weeks compared with CHF. Data are mean ± standard error; a (as reported above) and b ($p = 0.001$ for all groups) denote statistical significance of CHF vs NCM+3DFC and sham vs CHF respectively. Sham, $n = 8$ for all groups; CHF, $n = 20$ at 6 weeks, $n = 7$ at 10 weeks, $n = 6$ at 14 weeks, $n = 5$ at 18 weeks; and NCM-3DFC, $n = 26$ at 6 weeks, $n = 10$ at 10 weeks, $n = 9$ at 14 weeks, $n = 5$ at 18 weeks.

Table 1 Hemodynamic values 3 weeks after neonatal cardiomyocyte-3-dimensional fibroblast construct implantation in rats with chronic heart failure[a]

Group[b]	MAP (mm Hg)	SYS (mm Hg)	EDP (mm Hg)	CI (ml/[min × g])	dP/dt (+) (mm Hg/sec)	dP/dt (–) (mm Hg/sec)	Tau (ms)	PDP (mm Hg)
Sham	129 ± 4	128 ± 4	5 ± 1	0.52 ± 0.04	7146 ± 285	6368 ± 468	15 ± 1	171 ± 5
CHF	103 ± 4[c]	124 ± 5	27 ± 2[c]	0.45 ± 0.05	4651 ± 250[c]	2853 ± 148[c]	25 ± 1[c]	112 ± 8[c]
NCM-3DFC	100 ± 5	126 ± 4	15 ± 3[d]	0.61 ± 0.06[d]	5806 ± 192[d]	3517 ± 230[d]	21 ± 1[d]	146 ± 5[d]

CHF, chronic heart failure; CI, cardiac index; EDP, end diastolic pressure; MAP, mean arterial pressure; NCM-3DFC, neonatal cardiomyocyte–3-dimensional fibroblast construct; PDP, peak developed pressure; SYS, systolic pressure.

[a]Implantation of the NCM-3DFC improved EDP ($p = 0.002$), CI ($p = 0.015$), dP/dt(+) ($p = 0.002$), dP/dt (–) ($p = 0.031$), Tau ($p = 0.025$) and PDP ($p = 0.003$) compared with untreated CHF rats. Data are mean ± standard error.

[b]Sham: $n = 9$ (MAP), $n = 20$ (SYS), $n = 16$ (EDP), $n = 21$ (CI), $n = 17$ (dP/dt+), $n = 8$ (dP/dt–), $n = 8$ (Tau), $n = 7$ (PDP); CHF: $n = 10$ (MAP), $n = 12$ (SYS), $n = 9$ (EDP), $n = 7$ (CI), $n = 8$ (dP/dt+), $n = 10$ (dP/dt–), $n = 10$ (Tau), $n = 6$ (PDP); NCM-3DFC: $n = 13$ (MAP), $n = 12$ (SYS), $n = 9$ (EDP), $n = 9$ (CI), $n = 9$ (dP/dt+), $n = 12$ (dP/dt–), $n = 13$ (Tau), $n = 7$ (PDP).

[c]$p = 0.001$ for all groups denotes statistical significance of CHF vs NCM + 3DFC and sham vs CHF respectively.

[d]Values for p as reported above.

seeded cardiomyocytes in a manner allowing electromechan ical synchrony and thus the potential to track in sinus rhythm in vivo after implantation.

When implanted into rats with CHF and EFs below 35%, the NCM-3DFC improved ($p < 0.05$) LV function 3 weeks after implantation by increasing EF, cardiac index, dP/dt(+), dP/dt(–), and PDP, while lowering EDP and LV relaxation (Table 1). In addition, long-term improvements were also observed 18 weeks after implantation by increasing EF, MAP, dP/dt(+), dP/dt(–), and PDP (Table 2 and Figure 3). Implantations of the NCM-3DFC occurred 18 hours after culture to permit cardiomyocyte adhesion onto the 3DFC yet before the onset of spontaneous contractions and subsequent cellular organization, potentially allowing the underlying native myocardium to dictate organization in vivo. This may have contributed to the observation that all rats that received the NCM-3DFC maintained sinus rhythm with no observed arrhythmias. Echocardiographic data showed no LV dyssynchrony, supporting the observation that the patch does not alter local LV electrical-mechanical function (Figure 4). Furthermore, these findings demonstrate sustained functional improvements, not only over the short-term but long-term.

Although the mechanism of action in cell-based therapies have not been fully elucidated, it should be postulated that many contributory roles are at play that may include transplanted cell survival and paracrine-mediated effects that result in the observed reported functional benefits. Histologic evaluation at 3 and 18 weeks after implantations showed an increase in viable myocardium underneath the patch (Figure 4). This population of cells may be in part from the transplanted NCMs, endogenous cardiomyocyte migration, or enhancement of the native viable myocardium. Our previous work has shown that once implanted, the dermal fibroblasts embedded in the 3DFC secrete angiogenic cytokines, establishing microvascular support and increased blood flow.[20] The angiogenic cytokines may be supplementing and facilitating the survival of the transplanted cardiomyocytes.

These findings are exciting and support further evaluation of tissue-engineered scaffolds for therapeutic use to treat CHF, but limitations remain that must be overcome. Additional studies will have to be done developing a patch with a clinically relevant cell type. These cells need to be isolated with ease and in robust enough numbers to permit constructing patches. In addition, the concept of allogeneic vs autologous approaches needs to be addressed.

Table 2 Hemodynamic values 18 weeks after neonatal cardiomyocyte-3-dimensional fibroblast construct implantation in rats with chronic heart failure[a]

Group[b]	MAP (mm Hg)	SYS (mm Hg)	EDP (mm Hg)	CI (ml/[min × g])	dP/dt(+) (mm Hg/sec)	DP/dt(–) (mm Hg/sec)	Tau (ms)	PDP (mm Hg)
Sham	119 ± 2	119 ± 2	8 ± 1	0.35 ± 0.03	7,355 ± 400	6,103 ± 287	16 ± 1	178 ± 6
CHF	84 ± 2[c]	105 ± 7	28 ± 3[c]	0.32 ± 0.03	4,048 ± 217[c]	2,172 ± 130[c]	29 ± 1[c]	98 ± 9[c]
NCM-3DFC	101 ± 3[d]	111 ± 6	17 ± 7	0.33 ± 0.06	4,713 ± 118[d]	2,915 ± 219[d]	25 ± 2	137 ± 5[d]

CHF, chronic heart failure; CI, cardiac index; EDP, end diastolic pressure; MAP, mean arterial pressure; NCM-3DFC, neonatal cardiomyocyte–3-dimensional fibroblast construct; PDP, peak developed pressure; SYS, systolic pressure.

[a]Implantation of the NCM-3DFC improved MAP ($p = 0.003$), dP/dt(+) ($p = 0.05$), dP/dt(–) ($p = 0.043$) and PDP ($p = 0.02$) compared with untreated CHF rats. Data are mean ± standard error.

[b]Sham: $n = 8$ (MAP), $n = 8$ (SYS), $n = 8$ (EDP), $n = 8$ (CI), $n = 8$ (dP/dt+), $n = 8$ (dP/dt–), $n = 8$ (Tau), $n = 7$ (PDP); CHF: $n = 4$ (MAP), $n = 5$ (SYS), $n = 6$ (EDP), $n = 5$ (CI), $n = 5$ (dP/dt+), $n = 3$ (dP/dt–), $n = 3$ (Tau), $n = 3$ (PDP); NCM-3DFC: $n = 3$ (MAP), $n = 3$ (SYS), $n = 3$ (EDP), $n = 5$ (CI), $n = 3$ (dP/dt+), $n = 3$ (dP/dt–), $n = 3$ (Tau), $n = 3$ (PDP).

[c]$p = 0.001$ for all groups denotes statistical significance of CHF vs NCM+3DFC and sham vs CHF respectively.

[d]Values for p as reported above

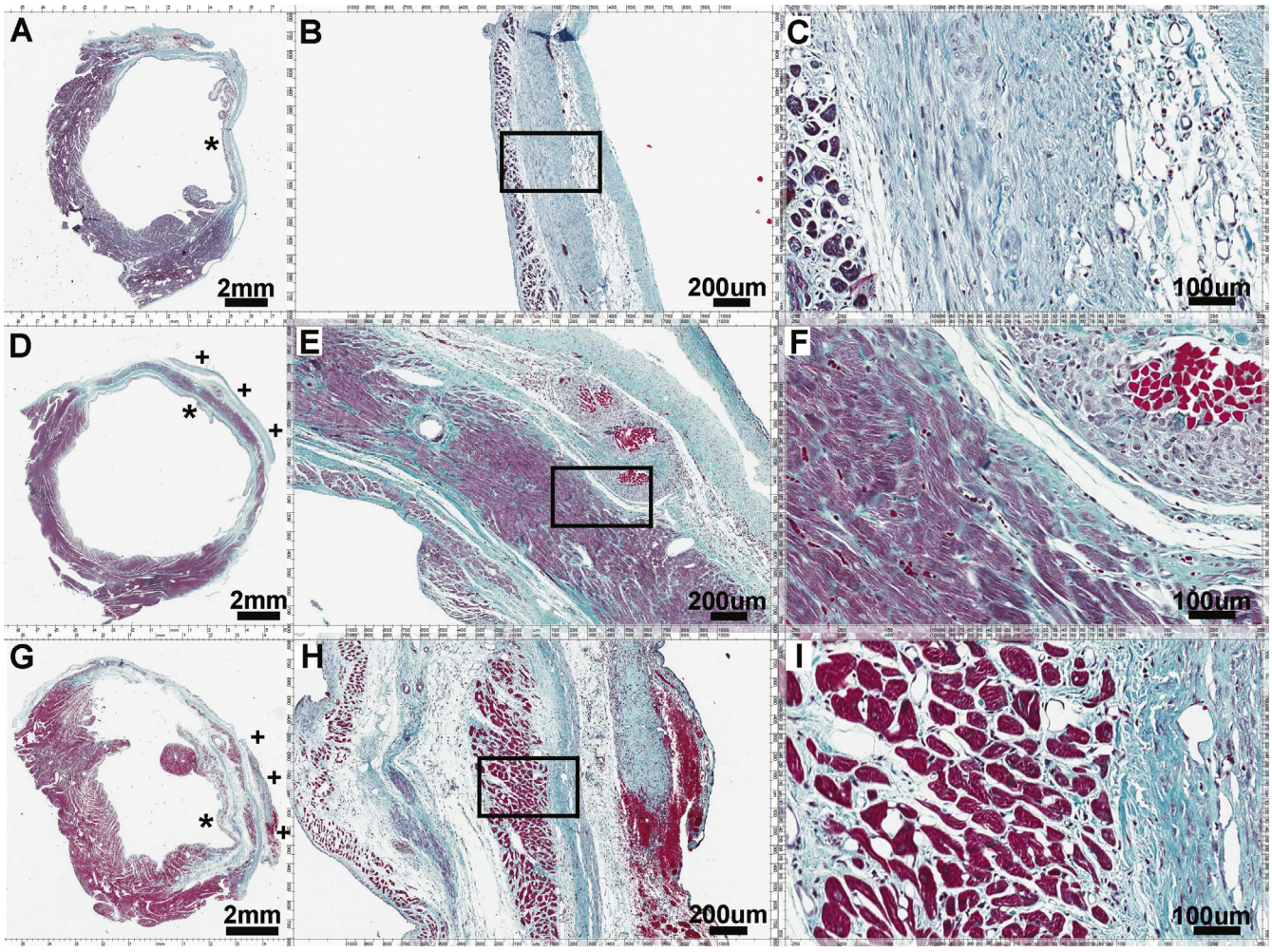

Figure 4 Trichrome-stained left ventricular cross sections of (A–C) 6-week chronic heart failure (CHF) control receiving an infarct but no treatment, (D–F) CHF + neonatal cardiomyocyte (NCM)–3-dimensional fibroblast construct (3DFC) 6 weeks after coronary artery ligation (3 weeks after implant), and (G–I) CHF + NCM-3DFC 21 weeks after coronary artery ligation (18 weeks after implant). Hearts were excised, and right ventricles were removed and cut in 5-μm transverse sections along the midpoint of the ventricle. Healthy myocardium is represented as red-purple, collagen/scar as blue, and red blood cells as small red dots. The * (A, D, and G) and box insets (B, E, H) represent area of corresponding higher magnification. The + in panel D and G highlights the location of the NCM-3DFC implant. Implantation of a cardiomyocyte patch results in increased LV wall thickness (D, E, G, H vs A and B) and preservation and/or generation of myocardium (D–F and G–I). The synthetic Vicryl (Ethicon, Somerville, NJ) components of the patch are degradable and not detectable after 3 weeks in vivo. (E and F) Remnants of the suture used for implantation of the NCM-3DFC can be seen as the bright red clusters.

In conclusion, this study demonstrates that a multicelluar, electromechanically organized, cardiomyocyte scaffold can be engineered in vitro by seeding and coculturing NCMs onto 3DFC. When implanted in a rat model of CHF, the NCM-3DFC improves short-term and long term LV function when evaluated using echocardiography and hemodynamics.

Disclosure statement

The authors acknowledge and thank Howard Byrne and Maribeth Stansifer, BS, for their technical work, and the SAVAHCS VA Biorepository for additional technical support and assistance. Histologic data were generated by the TACMASS Core (Tissue Acquisition and Cellular/Molecular Analysis Shared Service) and is supported by the Arizona Cancer Center Support Grant, National Institutes of Health CA023074.

This study was supported by the Department of Veteran Affairs, the William and Dorothy Shaftner Memorial Award–Sarver Heart Center, the Warmer Research Foundation, the Hansjörg Wyss Foundation, the Arizona Biomedical Research Commission, and the Biomedical Research and Education Foundation of Southern Arizona.

Theregen Inc, provided the 3DFC patch but did not provide any financial support for these studies. The University of Arizona had a Memorandum of Understanding with the Department of Veteran Affairs and has a licensing agreement with Theregen to use the 3DFC patch in the heart.

Dr Kellar was a consultant for Theregen. Dr Goldman was previously a non-paid member of the Scientific Advisory Board for Theregen. None of the other authors has a financial relationship with a commercial entity that has an interest in the subject of the presented manuscript or other conflicts of interest to disclose.

Supplementary data

Supplementary data are available in the online version of this article at www.jhltonline.org.

References

1. Srivastava D, Ivey KN. Potential of stem-cell-based therapies for heart disease. Nature 2006;441:1097-9.
2. Song K, Nam YJ, Luo X, et al. Heart repair by reporgramming non-myocytes with cardiac transcription factors. Nature 2012;485:599-604.
3. Tileman L, Ishikawa K, Weber T, Hajjar RJ. Gene therapy for heart failure. Circ Res 2012;110:777-93.
4. Schächinger V, Assmus B, Britten MB, et al. Transplantation of progenitor cells and regeneration enhancement in acute myocardial infarction: final one-year results of the TOPCARE-AMI Trial. J Am Coll Cardiol 2004;44:1690–1699.
5. Wollert KC, Meyer GP, Lotz J, et al. Intracoronary autologous bone-marrow cell transfer after myocardial infarction: the BOOST randomized controlled clinical trial. Lancet 2004;364:141-8.
6. Strauer BE, Brehm M, Zeus T, et al. Regeneration of human infarcted heart muscle by intracoronary autologous bone marrow cell transplantation in chronic coronary artery disease: the IACT Study. J Am Coll Cardiol 2005;46;1651–1658.
7. Assmus B, Honold J, Schachinger V, et al. Transcoronary transplantation of progenitor cells after myocardial infarction. N Engl J Med 2006;355:1222-32.
8. Janssens S, Dubois C, Bogaert J, et al. Autologous bone marrow-derived stem-cell transfer in patients with ST-segment elevation myocardial infarction; double blind, randomized controlled trial. Lancet 2006;367:113-21.
9. Lunde K, Solheim S, Aakhus S, et al. Intracoronary injection of mononuclear bone marrow cells in acute myocardial infarction. N Engl J Med 2006;355:1199-209.
10. Schächinger V, Erbs S, Elsässer A, et al. Intracoronary bone marrow-derived progenitor cells in acute myocardial infarction: a randomized, double-blind, placebo controlled multicenter trial (REPAIR-AMI). N Engl J Med 2006;355:1210-21.
11. Dow J, Simkhovich B, Kedes L, Kloner R. Wash-out of transplanted cells from the heart: a potential new hurdle for cell transplantation therapy. Cardiovasc Res 2005;67:301-7.
12. Müller-Ehmsen J, Whittaker P, Kloner RA, et al. Survival and development of neonatal rat cardiomyocytes transplanted into adult myocardium. J Mol Cell Cardiol 2002;34:107-16.
13. Zimmerman WH, Melnychenko I, Wasmeier G, et al. Engineered heart tissue grafts improve systolic and diastolic function in infarcted rat hearts. Nat Med 2006;12:452-8.
14. Sekine H, Shimizu T, Hobo K, et al. Endothelial cell coculture within tissue-engineered cardiomyocyte sheet enhances neovascularization. Circulation 2008;118(Suppl 1):S145-52.
15. Madden LR, Mortisen DJ, Sussman EM, et al. Proangiogenic scaffold as functional templates for cardiac tissue engineering. Proc Natl Acad Sci U S A 2010;107:15211-6.
16. Kellar RS, Landeen LK, Shephred BR, Naughton GK, Ratcliffe A, Williams SK. Scaffold-based 3-D human fibroblast culture provides a structural matrix that support angiogenesis in infarcted heart tissue. Circulation 2001;104:2063-8.
17. Kellar RS, Shepherd BR, Larson DF, Naughton GK, Williams SK. A cardiac patch constructed from human fibroblasts attenuates a reduction in cardiac function following acute infarct. Tissue Eng 2005;11:1678-87.
18. Fitzpatrick JR 3rd, Frederick JR, McCormick RC, et al. Tissue-engineered pro-angiogenic fibroblast scaffold improves myocardial perfusion and function and limits ventricular remodeling after infarction. J Thorac Cardiovasc Surg 2010;140:667-76.
19. Thai H, Juneman E, Lancaster J, et al. Implantation of a 3-dimensional fibroblast matrix improves left ventricular function and blood flow after acute myocardial infarction. Cell Transplant 2009;18:283-95.
20. Lancaster J, Juneman E, Hagerty T, et al. Viable fibroblast matrix patch induces angiogenesis and increases myocardial blood flow in heart failure after myocardial infarction. Tissue Eng Part A 2010;16:3065-73.
21. Camelliti P, Borg T, Kohl P. Structural and functional characterisation of cardiac fibroblasts. Cardiovasc Res 2005;65:40-51.
22. Camelliti P, Green C, Kohl P. Structural and functional coupling of cardiac myocytes and fibroblasts. Adv Cardiol 2006;42:132-49.
23. Liu H, Chen B, Lilly B. Fibroblast potentiate blood vessel formation partially through secreted factor TIMP-1. Angiogenesis 2008;11:223-34.
24. Aavula BR, Ali MA, Bednarczyk D, Wright SH, Mash EA. Synthesis and fluorescence of N,N,N-trimethyl-2-[methyl(7-nitrobenzo[c][1,2,5]oxadiazol-4-yl)amino]ethanaminium iodide, a pH-insensitive reporter of organic cation transport. Synthetic Comm 2006;36:701-5.
25. Ek-Vitorín JF, Burt JM. Quantification of gap junction selectivity. Am J Physiol Cell Physiol 2005;289:C1535-46.
26. He DS, Burt JM. Mechanism and selectivity of the effects of halothane on gap junction channel function. Circ Res 2000;86:E104-9.
27. Turner LA, Vodanovic S, Bosnjak ZJ. Interaction of anesthetics and catecholamines on conduction in the canine His-Purkinje system. Adv Pharmacol 1994;31:167-84.
28. Gaballa MA, Raya TE, Goldman S. Large artery remodeling after myocardial infarction. Am J Physiol 1995;268:H2092-103.
29. Raya TE, Gay RG, Aguirre M, Goldman S. The importance of venodilatation in the prevention of left ventricular dilatation after chronic large myocardial infarction in rats: a comparison of captopril and hydralazine. Circ Res 1989;64:330-7.
30. Raya TE, Gaballa M, Anderson P, Goldman S. Left ventricular function and remodeling after myocardial infarction in aging rats. Am J Physiol 1997;273:H2652-8.
31. Thai H, Do B, Tran T, Gaballa M, Goldman S. Aldosterone antagonism improves endothelial-dependent vasorelaxation in heart failure via upregulation of endothelial nitric oxide synthase production. J Card Fail 2006;12:240-5.
32. Thai H, Van H, Gaballa M, Goldman S, Raya T. Effects of AT1 receptor blockade after myocardial infarct on myocardial fibrosis, stiffness, and contractility. Am J Physiol 1999;276:H873-80.